Journal of Oleo Science
Copyright ©2023 by Japan Oil Chemists' Society
doi : 10.5650/jos.ess22389
J. Oleo Sci. **72**, *(9) 869-879 (2023)*

Nanoemulsion of the Essential Oil from *Blumea balsamifera* (L.) DC. and Its Effect on Trauma Repair

Guihua Liu[1,2], Jiankang Wang[2], Wen Zheng[2], Long Han[2], Jianming Huang[2], Zhangjiang He[1,2]*, and Jichuan Kang[1,2]*

[1] *College of Pharmacy, Guizhou University, Guiyang, Guizhou, People's Republic of CHINA*
[2] *Southwest Biomedical Resources of the Ministry of Education, Guizhou University, Guiyang, Guizhou, People's Republic of CHINA*

Abstract: The essential oil, extracted from the Hmong medicine *Blumea balsamifera* (L.) DC. (BBO), is a purely natural wound repair agent. Its application has, however, been restricted due to its low solubility and high volatility properties. In this study, we have developed a nanoemulsion formulation to improve the characteristics of BBO. The particle size of the nanoemulsion was normally distributed, and 71% of its range was concentrated between 10-100 nm, with an average particle size of 62.8 nm and an encapsulation rate of 98%. After 7 days of application, the wound healing rate of the BBO nanoemulsion (BBO-NE) group was 1.5 times higher than that of the normal BBO group. Along with histological observations, nanoemulsion formulation has been demonstrated to significantly improve the efficacy of BBO for wound repair. In addition, inflammation-related TLR4, CD14 and IRAK-1 gene transcript levels were significantly reduced after the administration of BBO-NE compared to the BBO group, with downregulation of 47.8%, 35.7% and 57.8%, respectively, while the secretion of pro-inflammatory factors IL-6 and TNF-α was also significantly reduced by 83.8% and 32.7%, respectively, in the nanoformulation administration (BBO-NE) group compared to the BBO group. In contrast, the anti-inflammatory factor IL-10 was significantly increased by 4.2-fold. It was further found that the drug penetration per unit area increased significantly 6.30% to 19.5% at different time points after the application of the BBO-NE compared to the BBO. In conclusion, nano-formulation enhanced the drug penetration of the BBO, reduced inflammatory factors, increased the level of anti-inflammatory factors, and promoted collagen deposition, thereby accelerating wound repair.

Key words: *Blumea balsamifera*, essential oil, nanoemulsion, wound repair, drug penetration

1 Introduction

Blumea balsamifera (L.) DC. is a perennial herb or subshrub of the Asteraceae family, a traditional Chinese Miao medicine with antiseptic, antioxidant and analgesic effects, and its main application form is the essential oil extracted from the plant. However, the oil is insoluble in water and highly volatile[1)], which makes it difficult to be used in practical applications because of the short duration of its efficacy and uncontrollable dosage. In order to improve the scope of medicinal use, preparations of *Blumea balsamifera* (L.) DC. essential oil (BBO) have been widely studied including tablets, semi-solid formulations and granules, which, however, have certain limitations and may cause irritation to the gastrointestinal tract and leading to symptoms such as nausea and vomiting. The BBO can only work slowly and is not suitable for emergency patients and patients with oral disorders[2)]. Nanoemulsions, as good carriers for lipophilic drugs, can improve drug solubility, fast absorption, high stability, and slow release targeting[3)], and are the ideal dosage form to address the application of BBO.

Studies have shown that topical application of BBO improves wound healing[4)]. *Via* enhancing the production of granulation in body tissues, it promotes the formation of new blood vessels, promoting epithelial deposition and wound contraction[5)]. Fatty acids, as important components of the essential oils, accelerate wound healing by reducing free radicals and scavenging reactive oxygen species, alter-

*Correspondence to: Jichuan Kang, College of Pharmacy, Guizhou University, Guiyang, Guizhou, People's Republic of CHINA. Zhangjiang He, College of Pharmacy, Guizhou University, Guiyang, Guizhou, People's Republic of CHINA
E-mail: jckang@gzu.edu.cn (JK), zjhe3@gzu.edu.cn (ZH)
Accepted June 18, 2023 (received for review November 22, 2022)
Journal of Oleo Science ISSN 1345-8957 print / ISSN 1347-3352 online
http://www.jstage.jst.go.jp/browse/jos/ http://mc.manusriptcentral.com/jjocs

ing the maturation and differentiation of the skin stratum corneum, affecting skin structure and immune status[6, 7]. Guaiacane sesquiterpenoids in essential oils have shown potential for wound healing *via* repairing damaged blood vessels[8]. In addition, flavonoids in the oils of traditional medicinal plants inhibit the exudation of inflammatory bioenzymes, reduce the inflammatory response of the body, and also enhance the wound healing effect[9]. L-Borneol and Caryophyllene are the main components of BBO, which can regulate skin permeability and exert anti-inflammatory and analgesic effects during wound repair[10–12]. Because of the diversity of the chemical composition of the BBO, fully exploring the BBO components as well as elucidating the mechanism of their action is awaiting further study.

In this study, we investigated the effects of nano-formulations of BBO on the skin wound repair. The results showed that the nano-formulations significantly enhanced skin absorption and promoted wound repair. In addition, it was found that in comparison with the BBO, the *Blumea balsamifera* (L.) DC. essential oil nanoemulsion (BBO-NE) not only intensified the down-regulation of gene transcription for inflammation and decreased the secretion of pro-inflammatory factors, but also increased the production of anti-inflammatory factors and promoted collagen deposition, and therefore accelerated wound repair. The results furthered the study on the molecular basis of the trauma repair of BBO, and demonstrated the strengthened effect of nano-emulsion on the trauma repair of BBO, which enriches the dosage form library of BBO and provides data support for the promotion and application of BBO.

2 Materials and Methods

2.1 Principal component analysis of BBO

The main chemical composition of BBO has been extensively resolved[13] (BBO, purity > 99%, purchased in Guizhou Ailikang Co., Ltd, China), and here we use Gas chromatography (GC, GC-2010, Shimadzu Corporation, Japan) to analyze the main components of essential oil (including L-borneol, L-camphor, pinene, linalool, β-caryophyllene, pepper oleoresin).

2.2 Preparation of BBO-NE

In this study, high energy emulsification method was used for the preparation of BBO-NE. The components including PCO40 (surfactant), anhydrous ethanol (co-surfactant), isopropyl myristate (oil phase) and distilled water (aqueous phase) were used for the preparation of the nanoemulsion[14], and the currently pending patent (BBO-NE in the preparation of antitumor drugs and wound repair drugs) gives detailed information about its preparation and optimization. Briefly, a prescribed amount of BBO and isopropyl myristate was weighed and mixed, a co-surfactant was added to dissolve the oil phase, then a certain amount of surfactant was added to the mixed system, and isopropyl myristate was weighed and mixed, a co-surfactant was added to dissolve the oil phase, then a certain amount of surfactant was added to the mixed system. The crude emulsion was obtained by adding distilled water dropwise while stirring. Finally the liquid preparation was emulsified with an ultrasonic pulverizer (ZOLLO-1800Y, Shanghai ZOLLO Instruments Co., Ltd, China) under ice bath conditions.

2.3 Measurement of particle size and calculation of encapsulation efficiency

Effective separation of free drug not encapsulated into nanoparticle carriers is essential for the calculation of encapsulation rate. Common separation methods include ultracentrifugation, dextran gel column method and dialysis method[15]. In the present study, the encapsulation rate was calculated using ultracentrifugation method *via* taking 2 mL of BBO-NE and centrifuging it at 13000 r/min for 30 min and then taking the supernatant as free drug donor. Likewise, equal amounts of BBO-NE were taken as the total drug donor, and the content of L-borneol (principal component of BBO) in both donor samples was determined by GC, and the encapsulation rate was calculated according to eq1. In addition, the nanoparticle properties and sizes were characterized and measured with transmission electron microscope (JEM-F200 field emission transmission electron microscope, Japan) and nanoparticle size measurement instrument (Nano ZSE, Malvern Panaco, UK), respectively.

$$EE = (1 - C_f/C_t) \times 100\% \quad \text{eq1}$$

Where EE is the encapsulation efficiency; C_f is the amount of free drug; C_t is the total amount of drug in the nanoemulsion suspension.

2.4 Stability assessment

The stability of the formulation was evaluated by examining the physical properties of the nanoemulsion under hot storage (45 ± 2℃), cold storage (4 ± 2℃) and room temperature (25 ± 2℃) conditions. The prepared BBO-NE was divided into three portions and placed in 4℃, 25℃ and 45℃ environments, and the samples were removed on the 10th and 20th day after placement to determine the pH, particle size and drug content[16].

2.5 *In vitro* drug release studies

In the present study *in vitro* drug release was performed in phosphate buffer (pH 7.4) with the help of dialysis bags (Chengdu Microcircuit Biotechnology Co., Ltd, China)[17]. The drug was loaded into the dialysis bag and the bag was placed in a beaker containing 100 mL dialysis solution. At specific time intervals, 1 mL of sample was

taken and the same volume of fresh buffer solution was added. The sample was filtered and the L-borneol content was determined using GC and the cumulative *in vitro* release was calculated, and the experiment was performed in triplicate.

2.6 Animal experiments

This thesis involves relevant animal experimental protocols all approved by the Animal Care and Use Committee of Guizhou University under the approval number EAE-GZU-2021-E017.

2.6.1 Skin irritation

(1) Experimental animals and grouping

The potential irritation of BBO and BBO-NE on normal and broken skin was studied using 200-250 g Wister rats (Tengxin Farm, Chongqing, China). Both normal and broken skin were divided into three dosing groups: BBO dosing group, BBO-NE dosing group and normal saline control group, with six animals in each group, half females (Both male and female are in good health and meet the basic requirements for follow-up research), randomly sampled (Normal skin group - the rats were fixed manually, and the area of 2 cm × 2 cm was dehaired with electric push scissors, and the skin was checked for damage before the experiment, and the injured skin was not used for the subsequent experiments; broken skin group - rats were anesthetized with 5% chloral hydrate solution and injected intraperitoneally at a dose of 0.5 mL/100 g. After entering anesthesia for about 2 min, a 2 cm × 2 cm area was debrided with electric push scissors. The 2 cm × 2 cm area was debrided and a sterile scalpel was used to form a "well" shaped wound in the debrided area, with slight blood leakage).

(2) Operation method

Normal saline was used as a control and each group was treated with 100 mg of the drug by applying it to the shaved area. After 24 h, the subject area was washed with warm water and the skin was carefully examined for signs of edema and erythema at the 1 h, 24 h, 48 h and 72 h after removal of the drug[18]. The irritation intensity of the drug was assessed by scoring according to the skin irritation criteria[19]. Each experimental group was raised in a single cage and labeled accordingly.

2.6.2 *In vivo* wound healing assessment

(1) Experimental animals and grouping

The trauma repair effects of BBO and BBO-NE were explored using 18-22 g KM mice (Tengxin Farm, Chongqing, China). Four administration groups were divided into blank group (No treatment done), BBO, BBO-NE and mupirocin (control group), with 8 animals in each group, half male and half female, randomly sampled.

(2) Operation method

After intraperitoneal injection with 1% chloral hydrate at a dose of 0.006 mL/g and entering anesthesia for about 2 min, the hair on the back of the mice was removed with a hair removal device, washed with warm water, disinfected locally with 5% iodine and 75% alcohol, and a circular wound with a diameter of 10 mm was cut at a symmetrical position of 10 mm on both sides of the back spine of the mice (with the help of a d = 10 mm skin punch, Guizhou Ruihong Biological Co., Ltd, China), without injuring the fascia and adipose tissue. The thickness of the myocardial wound was about 3 mm, and the wound was rinsed and disinfected with physiological saline. The wounds were opened, fully hemostatic, and kept in a single cage for observation for 24 h after awakening, during which they were free to drink and eat. The wounds were judged by the absence of bruising, swelling and suppuration, and the mice had normal feeding and good mobility, and they were included in the experimental groups as experimental subjects[20]. Each group was disinfected with iodine and saline daily, and the wound was changed once a day (no treatment was done for the blank group, and 100 mg was administered to the positive drug group, the BBO and the BBO-NE drug group), and the wound healing was observed by taking pictures on the first, third, fifth and seventh days of wound treatment, monitoring the changes of body weight and inflammatory factors and calculating the wound healing rate. Each experimental group was raised in a single cage and labeled accordingly.

$$\text{Healing rate} = (\text{original wound are} - \text{unhealed wound area})/\text{original wound area} \times 100\% \quad \text{eq2}$$

2.7 Skin permeation studies

(1) Skin pre-treatment

The mice were executed by cervical dislocation method, and the hair on the back of the mice was removed and the skin pieces of suitable size were cut and stored in the refrigerator at −80℃.

(2) Experimental operation

Amodified skin diffusion cell was used to carry out an *in vitro* permeation study of BBO and its nanoformulations[21]. The animal skin was immobilized on a donor chamber with a diffusion area of 2.0 cm^2 and the dermal side was in direct contact with the recipient chamber (100 mL). Phosphate buffer (pH = 5.8) was used as the diffusion medium and was continuously stirred at 37 ± 0.5℃ using magnetic beads (1500 r/min). Samples were withdrawn from the receiving chamber at different time intervals (0, 2, 4, 6, 8, 10, 12 and 24 h) and the withdrawn amounts were replaced with fresh phosphate buffer solution. The L-borneol content was determined using GC and the cumulative permeation was calculated.

2.8 Histological evaluation

At the end of the observation cycle of the drug skin trauma repair study, mice were executed using the cervical

dislocation method, and the circular wound and the surrounding 1-2 cm of animal skin were cut with surgical scissors for histological observation. The excised skin was fixed in 4% neutral formaldehyde, subjected to dehydration, wax immersion and embedding, sectioning, and dewaxing, and stained using acidic (eosin) and basic (hematoxylin) dyes for observation under the microscope[22], as well as for analysis of collagen deposition with the aid of Masson staining.

2.9 Determination of cytokines IL-6, TNF-α and IL-10 by ELISA

The 24-well plates were inoculated with mouse mononuclear macrophages (RAW264.7, purchased from Kunming Cell Bank, Chinese Academy of Sciences, China) at a cell density of 1×10^6 cells/mL. An amount of 500 μL of cell suspension was added to each well, and the cells were observed under an inverted microscope (IX-71, Olympus, Japan) to see whether they were evenly distributed. The cell culture plates were incubated at a temperature of 37℃ and with 5% CO_2 for 12 h. After the stimulation of inflammation by lipopolysaccharide (O55:B5, Sigma, USA), the drug was added for intervention[23], and the plates were placed in a 37℃ cell incubator (Thermo Fisher scientific, USA) for 12 h after administration; the cell supernatant was taken by centrifugation and other steps according to ELISA kits (Beijing Sizhengbai Biotechnology Co., Ltd, China) were used to determine Interleukin-6 (IL-6), tumor necrosis factor (TNF-α) and Interleukin-10 (IL-10) contents[24].

2.10 RNA extraction and RT-qPCR analysis

The 6-well plates were inoculated with RAW264.7 at a cell density of 1×10^6 cells/mL, 1.5 mL of cell suspension was added to each well, and the plates were incubated at a temperature of 37℃ and with 5% CO_2. Lipopolysaccharide was used to construct an *in vitro* inflammation model of macrophages[25], and RNA was extracted from each administration group with the help of RNA extraction kit (Beijing Kangwei Century Biotechnology Co., Ltd, China), which was used as a template after successful reverse transcription to examine the transcript levels of genes closely related to inflammation development including Toll-like receptor 4 (TLR4)[26], Leukocyte differentiation antigen (CD14)[27] and Interleukin-1 receptor-associated kinase (IRAK-1)[28].

2.11 Data analysis

All experimental data are expressed as the average of three independent replicates with the corresponding standard error (SE). One-way ANOVA was used to examine the findings of the qRT–PCR studies, the results of wound repair effect data, histological studies and drug permeation experiment for each sample were analyzed using t tests (and nonparametric tests), results with a significance level ($p<0.05$) were deemed statistically significant.

3 Results

3.1 Main chemical composition of BBO

The highest content of L-borneol was found in BBO, accounting for 46%, while the percentages of pepper oleoresin, L-camphor, β-caryophyllene, pinene and linalool in BBO were 5%, 10.2%, 5%, 2.5% and 0.1%, respectively (Fig. 1).

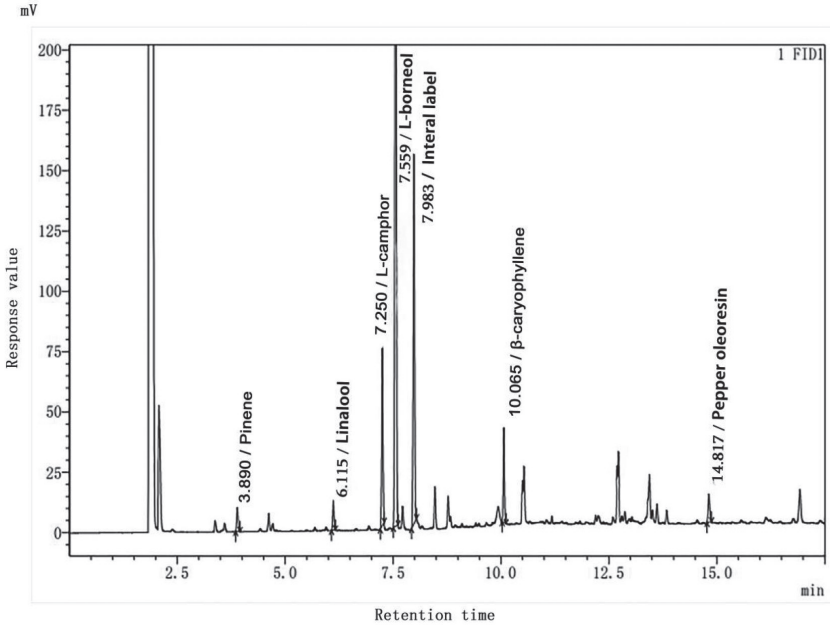

Fig. 1 Chromatogram of BBO composition analysis.

3.2 Physicochemical properties of BBO-NE

The BBO-NE was prepared by high-energy emulsification method. It was found that the empty carrier was white and transparent, while the BBO-NE was yellow and transparent with high optical transparency (Fig. 2a). Transmission electron microscopy revealed that the BBO-NE had a relatively regular spherical shape, and the droplets were uniformly distributed without adhesion and aggregation (Fig. 2b). The particle size showed a normal distribution pattern, with 71% of the distribution range concentrated in the range of 10-100 nm, and the average particle size was about 62.8 nm (Fig. 2c). The thermodynamic stability test showed that temperature did not significantly affect the pH (Fig. 2d), droplet size (Fig. 2e) and drug content (Fig. 2f), where the droplet size was basically unchanged and the drug content remained above 92.8% under the storage conditions of 4℃ and 25℃. Under storage conditions of 45℃, the pH value slightly decreases, which may be caused by the hydrolysis of some fatty acids in the oil phase. The above results indicated that the indexes of all parameters of the BBO-NE prepared *via* the high-energy emulsification method met the basic requirements of nanoemulsion dosage forms[16].

3.3 Nanoemulsion of BBO enhances the wound repair

To investigate the trauma repair effect of BBO-NE, a mouse trauma model was constructed. The skin irritation test revealed that there was no significant change in both normal and broken skin after application of BBO and its nanoemulsion compared with the negative control group (Fig. S1), and combined with the irritation scores (Table SI), it indicated that BBO and its nanoemulsion had no skin irritation and were suitable for skin application. The wound healing test revealed that the area of traumatized tissue gradually decreased in each group as the feeding period was extended (Fig. 3a). A gradual increase in body weight in each experimental group means that the experimental mice are in relatively good physical condition (Fig. 3b). On day 3 of wound treatment, the healing rate of the mupirocin group was significantly higher compared with the blank control group, about 1.6 times that of the control group, and there was no significant difference between the BBO group and the BBO-NE group, about 1.3 times of that of the control group. On day 5 of wound treatment, there was no significant difference of the wound healing rate between the BBO group and the mupirocin group, while the healing rate of the BBO-NE group was about 1.2 times of those of the other two groups (Figs. 3a and 3c). On day 7 of wound treatment, the wound healing rates of the positive drug group, the BBO group and the BBO-NE group were 70.4%, 74.5% and 85.1%, respectively, which indicated that the BBO-NE group was significantly higher than those of the other two groups. This indicates that the nanoemulsion formulation improved the wound healing ability of BBO.

To investigate the reason for the nanoemulsion form to improve the wound healing ability of BBO, we performed tissue observation of the wounds on the 7th day of wound healing. It was found that both the administrations of the drug caused a decrease in the number of inflammatory

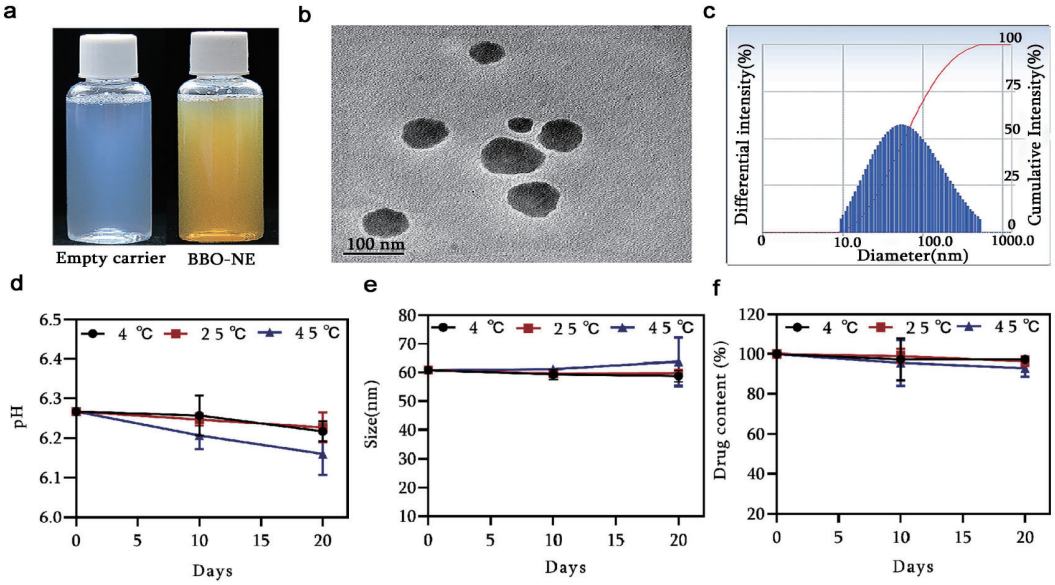

Fig. 2 Evaluation of the appearance and stability of BBO-NE: (a) Appearance of empty carrier and BBO-NE; (b) Transmission electron microscope of BBO-NE; (c) Particle size distribution of BBO-NE; (d) Changes in pH of BBO-NE stored at 4℃, 25℃ and 45℃ for 20 days; (e) Changes in particle size of BBO-NE stored at 4℃, 25℃ and 45℃ for 20 days; (f) Changes in drug content of BBO-NE stored at 4℃, 25℃ and 45℃ for 20 days.

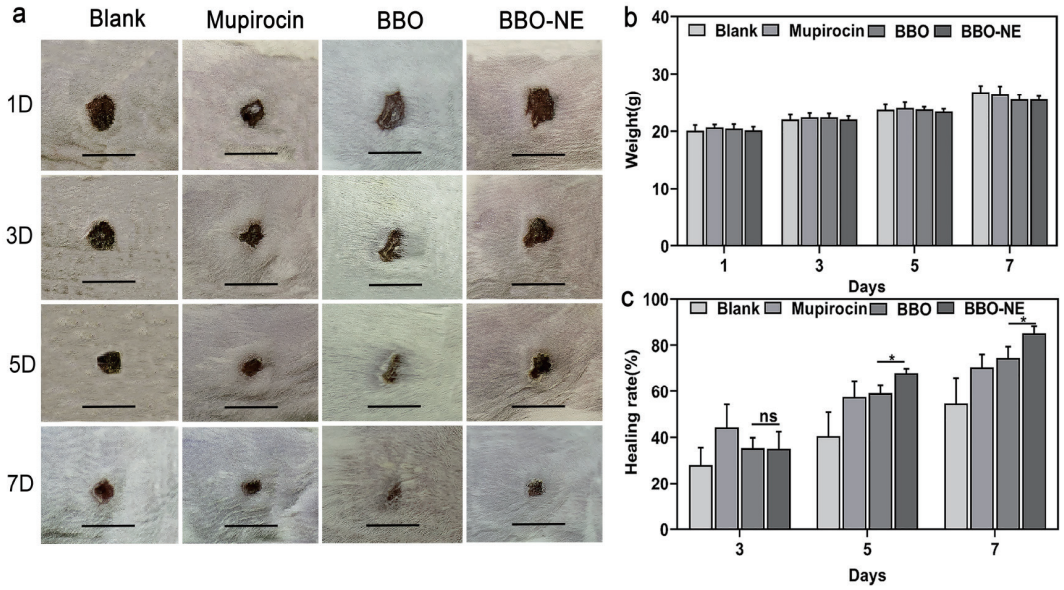

Fig. 3 Nanoemulsion form enhances the wound repair effect of BBO: (a) Representative images of wound healing. Scale bar: 10 mm; (b) Observed changes in body weight of animals in each experimental group on days 1, 3, 5, and 7 after wound treatment; (c) Changes in wound healing rate of each experimental group on days 3, 5, and 7 after wound treatment; results are given as means ± SE from three biological replicates, ns represents no significant difference, *$p < 0.05$.

cells compared to the blank group (Fig. 4a). The positive control group showed no significant difference in the number of inflammatory cells compared to the BBO-NE group, but was significantly lower than the BBO group, with a 44.3% decrease (Fig. 4b). Collagen deposition was observed to be increased in the drug administration group. The maximum positive drug collagen deposition was about 2.10 times higher than that of the blank group, while the BBO-NE group showed a increase in collagen deposition of about 3.7% compared to the BBO group (Figs. 4c and 4d). Thus, it is speculated that the nano-formulation increases the wound repair efficacy of BBO *via* reducing the number of inflammatory cells and increasing collagen production.

3.4 The BBO-NE accelerates inflammation reduction

To investigate the mechanism for the decrease in inflammation accelerated by the BBO-NE, the transcript levels of inflammation-related genes viz TLR4, CD14 and IRAK-1 were examined. The results revealed that the three genes were significantly downregulated after the treatments of either BBO or BBO-NE at all the concentrations (Figs. 5a, 5b and 5c). At 5 μg/mL and 10 μg/mL concentrations, the transcript levels of TLR4, CD14 and IRAK-1 were significantly down-regulated in the BBO-NE group compared to the BBO group by 47.8%, 47.7%, 35.7% and 32.0%, 34.1%, 57.8% ($p < 0.05$), respectively. While at 20 μg/mL concentration, only the transcript level of TLR4 were significantly reduced 36.2% (Fig. 5a), the transcript levels of CD14 and IRAK-1 were not significantly different between both groups (Figs. 5b and 5c). We also examined the levels of inflammatory factors viz IL-6 and TNF-α and anti-inflammatory factor viz IL-10. The results showed that after the application of 5 μg/mL of BBO and BBO-NE, the levels of IL-6 and TNF-α were significantly reduced compared to the control group, but no significant difference between the two groups (Figs. 5d and 5e). At the concentrations of 10 μg/mL and 20 μg/mL, the levels of IL-6 and TNF- α were significantly reduced in the BBO-NE group compared with the BBO group by 39.0%, 83.8% and 32.7%, 57.0% ($p < 0.05$) respectively. Meanwhile the trend of the anti-inflammatory factor IL-10 was exactly opposite to the inflammatory factor, with a significant 2.15-4.17-fold increase of IL-10 in the BBO-NE group compared to the BBO group after the treatments of 5, 10 and 20 μg/mL (Fig. 5f). Based on these results, it is speculated that BBO-NE did not actually alter the mechanisms associated with the anti-inflammatory properties of the BBO, however accelerated skin wound healing *via* exacerbating the reduction of inflammatory factors and enhancing the production of anti-inflammatory factors.

3.5 BBO-NE to promote the release and absorption of BBO

To investigate how the nano-formulations accelerate wound healing, skin absorption and drug release tests were conducted on both formulations. It was found that there was no significant change in the drug release rate of both BBO and BBO-NE at the first 10 h. However, at 12 h after

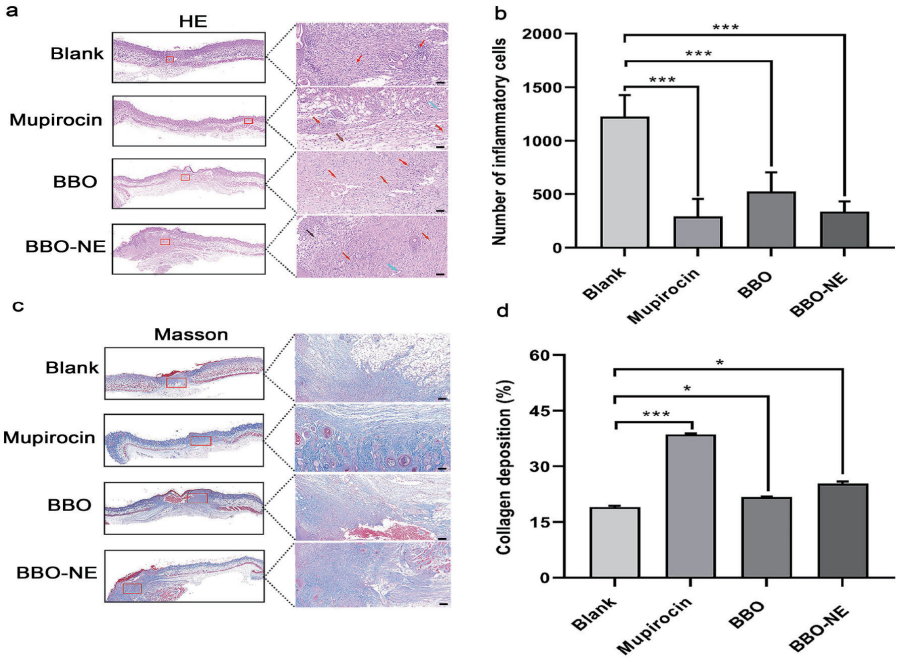

Fig. 4 Histopathological images of wound tissue: (a) Representative images of HE: the red arrow represents inflammatory cell infiltration, the brown arrow represents subcutaneous tissue edema and loose connective tissue arrangement, the purple arrow represents mild hemorrhage, and the blue arrow represents neovascularization, scale bar: 50 μm; (b) Statistical analysis of the number of inflammatory cells; results are given as means ± SE from three biological replicates, ***$p < 0.01$; (c) Representative images of Masson; scale bar : 50 μm; (d) Statistical analysis of collagen deposition; *$p < 0.05$, ***$p < 0.01$.

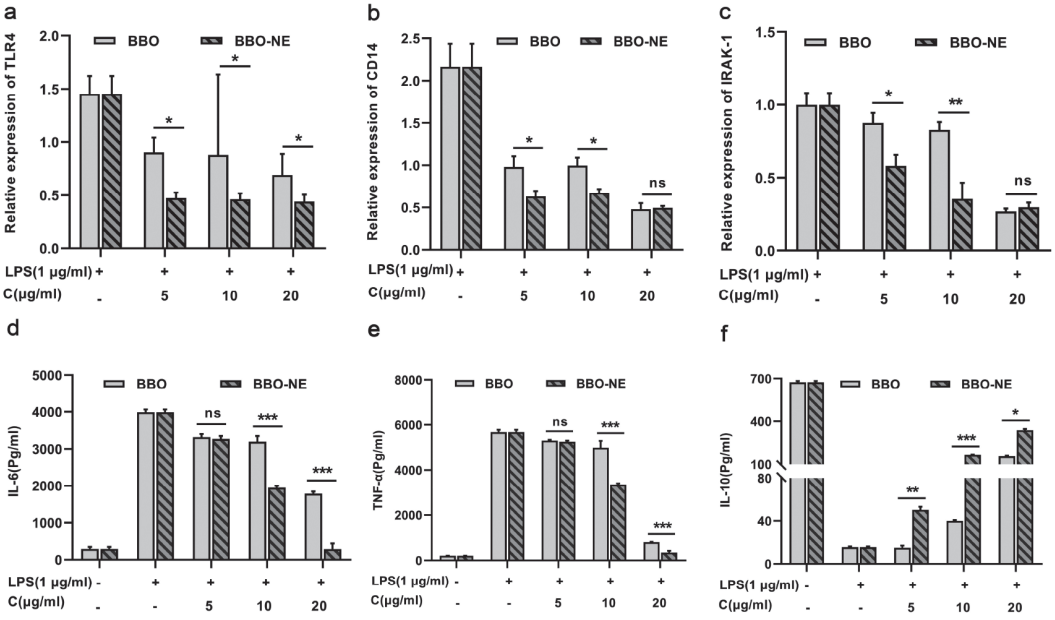

Fig. 5 ELISA and RT-qPCR measurements: (a) The RNA expression of TLR4; (b) CD14; (c) IRAK-1; (d) Reduction in IL-6 production after treatment of cells with BBO / BBO-NE (5-20 μg/mL); (e) Reduction in TNF-α production after treatment of cells with BBO / BBO-NE (5-20 μg/mL); (f) Levels of IL-10 were increased, compared with LPS stimulation; "c" represents the concentration of drug applied to cells; "+" represents administration, and "-" represents no administration; results are given as means ± SE from three biological replicates, ns represents no significant difference, *$p < 0.05$, **$p < 0.01$, ***$p < 0.005$.

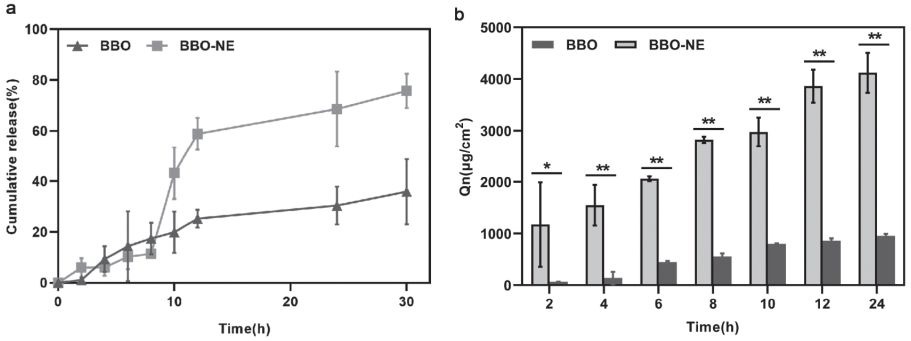

Fig. 6 *In vitro* drug release and transdermal absorption: (a) Changes *in vitro* drug release rate of BBO and BBO-NE at 0, 2, 4, 6, 8, 10, 12, 24, 30 h; (b) Changes in drug permeation per unit area from 2 h to 24 h after drug transdermal; results are given as means ± SE from three independent replicates, $*p<0.01$, $**p<0.001$.

application, the cumulative release rate of BBO-NE was 58.8%, which was much higher than that of the BBO (25.2%), and during the 12-30 h period, the BBO-NE increased from 58.8% to 75.7%, while the BBO increased from 25.2% to 35.9% only (Fig. 6a). This indicates that BBO-NE has a higher drug release rate than the BBO. Meanwhile the drug penetration measurements showed that the drug penetration increased gradually from 2-24 h after drug application (Fig. 6b). From the 10th to 30th hour after drug administration, the drug permeability of BBO-NE increased by 6.30% to 19.5% compared to the BBO group ($p<0.05$). It is hypothesized that the nanoemulsion dosage form facilitated the release and penetration of the drug by changing the delivery mode of the drug, leading to an increase in the accumulation of effective drug at the trauma site.

4 Discussion

In recent years, studies based on the activity of BBO have focused on antibacterial[29], antioxidant[30] and promotion of skin wound healing[31]. However, the complex composition and mechanism of action of BBO are not yet fully understood, leading to more topical applications. The volatility and low dissolution rate of BBO limit the application of BBO by direct application. Therefore, the development of suitable dosage forms to improve the efficacy of BBO is an effective way to solve the problem.

In this study, a nanoemulsion of BBO was successfully developed by using a nano-emulsion drug delivery system with good thermodynamic stability. It was found that the wound repair effect of the BBO-NE was higher than that of the marketed drug mupirocin cream and BBO, indicating that the nanoemulsion delivery system improved the efficacy of BBO. In addition, we constructed an *in vitro* cellular inflammation model by treating mononuclear macrophages with lipopolysaccharide to explore the effects of the BBO and the BBO-NE on inflammatory cells. We found that the treatment of BBO significantly reduced the occurrence of inflammation in cells, while BBO-NE further reduced the level of inflammation, mainly *via* a significant reduction in inflammatory factors and a significant increase in anti-inflammatory factor. This suggests that the nanoemulsion form does not change the anti-inflammatory mechanism of action of BBO, but enhances the effect to a higher level. However, from the tissue observation results we found that the number of inflammatory cells in the positive drug group was lower than that in the BBO-NE group, and collagen deposition was higher than that in the BBO-NE group, while the wound healing rate was lower than that in the BBO-NE group. We therefore speculate that there may be some other mechanisms of wound repair in BBO that are unknown to us.

L-Borneol is the main component of BBO[32, 33], which has many pharmacological activities, such as anti-inflammatory[34], analgesic[35], sedative[36], and anti-bacterial[37], these activities help BBO play a role in wound healing. As a complex[38], the combination of various ingredients of BBO may also have numerous mysterious offensive effects like other Chinese medicine[39]. Also, our data showed that at an action concentration of 5 μg/mL, there was already a difference in the transcript levels of inflammation-related genes between the BBO group and the BBO-NE group, but no difference in the levels of inflammatory and anti-inflammatory factors at the same concentration, indicating a certain concentration relationship between inflammatory genes and inflammatory and anti-inflammatory factors, and this result provides a minimum dosage guideline for the treatment of the BBO-NE.

The most important characteristic of nanoemulsion dosage form is that the particles are nanoscale in diameter, and the general size of nanoparticles is in the range of 10.0-100 nm, which means that with a larger surface area, it has a higher drug permeability compared to other dosage forms[40, 41]. Our experimental results revealed that most of the diameters of the BBO-NE were concentrated in the range of 50-100 nm, which perfectly fits the size range of

nanoemulsion dosage forms with an effective encapsulation rate of 98.0%, and these properties will greatly improve the medicinal efficiency of the BBO. The results of drug release rate test showed that the drug release rate of nanoemulsion dosage form could reach 75.7%, while that of the BBO group was only 35.9%. This indicates that the nanoemulsion dosage form can improve the medicinal efficiency of the BBO. The reason for the low release rate of the BBO may be due to its own high volatility, while it is possible that the nanoemulsion dosage form changes the drug delivery method and limits the volatilization of the BBO. In addition, the presence of lipids in the composition of nanoemulsions can effectively cross the skin stratum corneum barrier and enhance drug absorption and thus drug bioavailability[42, 43]. The results of the study showed that the drug absorption rate per unit area was significantly higher in the BBO-NE group than in the control group.

5 Conclusion

The nanoemulsion form of BBO accelerates the removal of inflammatory factors from wounds and accelerates collagen deposition by increasing the release rate and skin absorption of BBO, resulting in an increased amount of effective drug per unit area for the same amount of drug action, which in turn shortens wound healing time.

Acknowledgements

Many thanks to the National Natural Science Foundation of China (Nos. 32170019; 32160667; 31901947) for their support and everyone who contributed to our research.

Author Contributions

JK and ZH conceived of and designed the experiments. GL performed the experiments, analyzed the data, and contributed to the manuscript preparation and editing. JW and JH prepared the material for animal experiments. WZ and LH prepared the material for cell experiments. All authors have read and approved the manuscript.

Supporting Information

This material is available free of charge *via* the Internet at doi: 10.5650/jos.ess22389

Declarations

Ethics Approval

The relevant animal experimental protocols were all approved by the Animal Care and Use Committee of Guizhou University under approval number EAE-GZU-2021-E017.

Conflict of Interest

The authors declare no competing interests.

Data Availability Statement

All material and data are stored at Guizhou University, College of Pharmacy, Guiyang, People's Republic of China, and may be shared upon request directed to the corresponding author.

References

1) Wang, Y.H.; Zhang, Y.R. Variations in compositions and antioxidant activities of essential oils from leaves of Luodian *Blumea balsamifera* from different harvest times in China. *PLoS One* **15**, e0234661 (2020).
2) Feng, J.; Gao, M.; Zhao, C.; Yang, J.; Gao, H. *et al.* Oral administration of probiotics reduces chemotherapy-induced iarrhea and oral mucositis: A systematic review and meta-analysis. *Front. Nutr.* **9**, 823288 (2022).
3) Fan, Z.-W.; Pang, Y.-X.; Wang, K.; Yu, F.-L.; Wang, D. *et al. Blumea balsamifera* oil for the acceleration of healing of burn injuries. *Molecules* **20**, 17166-17179 (2015).
4) Silva, J.R.; Burger, B.; Kühl, C.M.C.; Candreva, T.; dos Anjos, M.B.P.; Rodrigues, H.G. Wound healing and omega-6 fatty acids: From inflammation to repair. *Mediators Inflamm.* **2018**, 1-17 (2018).
5) Huchzermeyer, B.; Menghani, E.; Khardia, P.; Shilu, A. Metabolic pathway of natural antioxidants, antioxidant enzymes and ROS providence. *Antioxidants* **11**, 761 (2022).
6) Gao, T.; Zhang, Y.; Shi, J.; Mohamed, S.R.; Xu, J.; Liu, X. The antioxidant guaiacol exerts fungicidal activity against fungal growth and deoxynivalenol production in *Fusarium graminearum. Front. Microbiol.* **12**, 762844 (2021).
7) Kakar, M.; Amin, M.U.; Alghamdi, S.; Sahibzada, M.U.K.; Ahmad, N.; Ullah, N. Antimicrobial, cytotoxic, and antioxidant potential of a novel flavone "6,7,4′-trimethyl flavone" isolated from *Wulfenia amherstiana. Evid. Based Complementary Altern. Med.* **2020**, 1-12 (2020).
8) Cao, W.; Zhai, X.; Ma, J.; Fu, X.; Zhao, B. *et al.* Natural borneol sensitizes human glioma cells to cisplatin-induced apoptosis by triggering ROS-mediated oxidative damage and regulation of MAPKs and PI3K/AKT pathway. *Pharm. Biol.* **58**, 72-79 (2020).
9) Xin, Y.; Zhao, H.; Xu, J.; Xie, Z.; Li, G. *et al.* Borneol-modified chitosan: Antimicrobial adhesion properties

and application in skin flora protection. *Carbohydr. Polym.* **228**, 115378(2020).
10) Di Sotto, A.; Maffei, F.; Hrelia, P.; Castelli, F.; Sarpietro, M.G.; Mazzanti, G. Genotoxicity assessment of β-caryophyllene oxide. *Regul. Toxicol. Pharmacol.* **66**, 264-268(2013).
11) Wang, Y.H.; Yu, X.Y. Biological activities and chemical compositions of volatile oil and essential oil from the leaves of *Blumea balsamifera*. *J. Essent. Oil-Bear. Plants* **21**, 1511-153(2018).
12) Algahtani, M.S.; Ahmad, M.Z.; Nourein, I.H.; Albarqi, H.A.; Alyami, H.S. *et al.* Preparation and characterization of curcumin nanoemulgel utilizing ultrasonication technique for wound healing: *In vitro*, *ex vivo*, and *in vivo* evaluation. *Gels* **7**, 213(2017).
13) Schultz, J.; Kirner, F.; Potapov, P.; Büchner, B.; Lubk, A.; Sturm, E.V. Tailoring plasmonics of Au@Ag nanoparticles by silica encapsulation. *Adv. Opt. Mater.* **9**, 2101221(2021).
14) Wang, C.; Wang, M.; Chen, P.; Wang, J.; Le, Y. Dasatinib nanoemulsion and nanocrystal for enhanced oral drug delivery. *Pharmaceutics* **14**, 197(2022).
15) Yu, W.P.; Wong, J.P.; Chang, T.M.S. Sustained drug release characteristics of biodegradable composite poly (d,l)lactic acidpoly(I)lactic acid microcapsules containing ciprofloxacin. *Artif. Cells Blood Substit. Biotechnol.* **28**, 39-55(2000).
16) Wolfe, M.K.; Wells, E.; Mitro, B.; Desmarais, A.M.; Scheinman, P.; Lantagne, D. Seeking clearer recommendations for hand hygiene in communities facing Ebola: A randomized trial investigating the impact of six handwashing methods on skin irritation and dermatitis. *PLoS One* **11**, e0167378(2016).
17) Hussain, A.; Samad, A.; Singh, S.K.; Ahsan, M.N.; Haque, M.W. *et al.* Nanoemulsion gel-based topical delivery of an antifungal drug: *In vitro* activity and *in vivo* evaluation. *Drug Deliv.* **23**, 642-657(2016).
18) Amoozegar, H.; Ghaffari, A.; Keramati, M.; Ahmadi, S.; Dizaji, S. *et al.* A novel formulation of simvastatin nanoemulsion gel for infected wound therapy: *In vitro* and *in vivo* assessment. *J. Drug Deliv. Sci. Technol.* **72**, 103369(2021).
19) Chakraborty, T.; Gupta, S.; Nair, A.; Chauhan, S.; Saini, V. Wound healing potential of insulin-loaded nanoemulsion with aloe vera gel in diabetic rats. *J. Drug Deliv. Sci. Technol.* **64**, 102601(2021).
20) Ahmad, N.; Ahmad, R.; Al-Qudaihi, A.; Alaseel, S.E.; Fita, I.Z. *et al.* Preparation of a novel curcumin nanoemulsion by ultrasonication and its comparative effects in wound healing and the treatment of inflammation. *RSC Adv.* **9**, 20192-20206(2019).
21) De Bus, I.; van Krimpen, S.; Hooiveld, G.J.; Boekschoten, M.V.; Poland, M. *et al.* Immunomodulating effects of 13- and 16-hydroxylated docosahexaenoyl ethanolamide in LPS stimulated RAW264.7 macrophages. *Biochim. Biophys. Acta - Mol. Cell Biol. Lipids* **1866**, 158908(2021).
22) Olajide, O.A.; Akande, I.S.; da Silva Maia Bezerra Filho, C.; Lepiarz-Raba, I.; de Sousa, D.P. Methyl 3,4,5-trimethoxycinnamate suppresses inflammation in RAW264.7 macrophages and blocks macrophage–Adipocyte interaction. *Inflammopharmacol.* **28**, 1315-1326 (2020).
23) Xu, Y.; Huang, Y.; Cai, S. Characterization and function analysis of interleukin-1 receptor-associated kinase-1 (IRAK-1)from *Fenneropenaeus penicillatus*. *Fish Shellfish Immunol.* **61**, 111-119(2017).
24) Wang, X.; Pham, A.; Kang, L.; Walker, S.A.; Davidovich, I. *et al.* Effects of adipose-derived biogenic nanoparticle-associated microRNA-451a on toll-like receptor 4-induced cytokines. *Pharmaceutics* **14**, 16(2021).
25) Roedig, H.; Nastase, M.V.; Frey, H.; Moreth, K.; Zeng-Brouwers, J. *et al.* Biglycan is a new high-affinity ligand for CD14 in macrophages. *Matrix Biol.* **77**, 4-22 (2019).
26) Su, Q.; Lv, X.; Ye, Z.; Sun, Y.; Kong, B. *et al.* The mechanism of MiR-142-3p in coronary microembolization-induced myocardiac injury *via* regulating target gene IRAK-1. *Cell Death Dis.* **10**, 61(2017).
27) He, C.; Yang, P.; Wang, L.; Jiang, X.; Zhang, W. *et al.* Antibacterial effect of *Blumea balsamifera* DC. essential oil against *Haemophilus parasuis*. *Arch. Microbiol.* **202**, 2499-2508(2020).
28) Ginting, B. Biosynthesis copper nanoparticles using *Blumea balsamifera* leaf extracts: Characterization of its antioxidant and cytotoxicity activities. *Surf. Interfaces* **7**, 100799(2020).
29) Pang, Y.; Wang, D.; Fan, Z.; Chen, X.; Yu, F. *et al.* *Blumea balsamifera*—A phytochemical and pharmacological review. *Molecules* **19**, 9453-9477(2014).
30) Ma, R.; Su, P.; Ma, Q.; Guo, J.; Chen, S. *et al.* Identification of(-)-Bornyl diphosphate synthase from *Blumea balsamifera* and its application for(-)-borneol biosynthesis in *Saccharomyces cerevisiae*. *Synth. Syst. Biotechnol.* **7**, 490-497(2022).
31) Wang, Y.-H.; Tian, H.-Y.; Wang, A.-M.; Wang, H.-X.; Zou, C.-L. A green and solvent-free process for preparation of high-purity(–)-borneol from leaves of *Blumea balsamifera*(L)DC. *Trop. J. Pharm Res.* **13**, 41(2014).
32) Yu, F.-L.; Zhao, N.; Wu, Z.-S.; Huang, M.; Wang, D. *et al.* NIR Rapid assessments of *Blumea balsamifera* (Ai-Na-Xiang)in China. *Trop. J. Pharm Res.* **22**, 1730 (2017).
33) Widhiantara, I.G.; Jawi, I.M. Phytochemical composition and health properties of Sembung plant(*Blumea balsamifera*): A review. *Vet. World* **14**, 1185-1196 (2021).
34) Sousa, D.P.; Raphael, E.; Brocksom, U.; Brocksom, T.J.

Sedative effectof monoterpene alcohols in mice: A preliminary screening. *J. Biosci.* **62**, 563(2007).
35) Chen, Z.; Xu, Q.; Shan, C.; Shi, Y.; Wang, Y.; Chang, R.C. Borneol for regulating the permeability of the blood-brain barrier in experimental ischemic stroke: Preclinical evidence and possible mechanism. *Oxidative Med.* **2019**, 1-15(2019).
36) Cao, W.; Zhai, X.; Ma, J.; Fu, X.; Zhao, B. *et al.* Natural borneol sensitizes human glioma cells to cisplatin-induced apoptosis by triggering ROS-mediated oxidative damage and regulation of MAPKs and PI3K/AKT pathway. *Pharm. Biol.* **58**, 72-79(2020).
37) Ji, J.; Zhang, R.; Li, H.; Zhu, J.; Pan, Y.; Guo, Q. Analgesic and anti-inflammatory effects and mechanism of action of borneol on photodynamic therapy of acne. *Environ. Toxicol. Pharmacol.* **75**, 103329(2020).
38) Shakeel, F.; Shazly, G.A.; Raish, M.; Ahmad, A.; Kalam, M.A. *et al.* Biological investigation of a supersaturated self-nanoemulsifying drug delivery system of *Piper cubeba* essential oil. *RSC Adv.* **5**, 105206-105217 (2015).
39) Jain, S.; Kambam, S.; Thanki, K.; Jain, A.K. Cyclosporine A loaded self-nanoemulsifying drug delivery system(SNEDDS): Implication of a functional excipient based Co-encapsulation strategy on oral bioavailability and nephrotoxicity. *RSC Adv.* **5**, 49633-49642(2015).
40) Vaz, G.R.; Carrasco, M.C.F.; Batista, M.M.; Barros, P.A.B.; Oliveira, M. da C. *et al.* Curcumin and quercetin-loaded lipid nanocarriers: Development of omega-3 mucoadhesive nanoemulsions for intranasal administration. *Nanomaterials* **12**, 1073(2022).
41) Khan, R.; Shah, S.; Rashid, S.; Naseem, F.; Shah, K. *et al.* Lornoxicam-loaded chitosan-decorated nanoemulsion: Preparation and *in vitro* evaluation for enhanced transdermal delivery. *Polymers* **14**, 1922(2022).
42) Liu, C.; Hu, J.; Sui, H.; Zhao, Q.; Zhang, X.; Wang, W. Enhanced skin permeation of glabridin using eutectic mixture-based nanoemulsion. *Drug Deliv. Transl. Res.* **7**, 325-332(2017).
43) Khan, R.; Shah, S.; Rashid, S.; Naseem, F.; Shah, K. *et al.* Lornoxicam-loaded chitosan-decorated nanoemulsion: Preparation and *in vitro* evaluation for enhanced transdermal delivery. *Polymers* **14**, 1922(2022).